Hindawi
International Journal of Aerospace Engineering
Volume 2021, Article ID 8838784, 9 pages
https://doi.org/10.1155/2021/8838784

Review Article

Adaptive Fixed-Time Nonsingular Terminal Sliding Mode Attitude Tracking Control for Spacecraft with Actuator Saturations and Faults

Zhiguo Han,[1] Minghao Wang,[2] Xunliang Yan ,[1] and Hang Qian[3]

[1] *School of Astronautics, Northwestern Polytechnical University, Xi'an Shaanxi 710072, China*
[2] *Institute of Survival Technology Effectiveness Evaluation of Flying Vehicle, Beijing 100085, China*
[3] *Beijing Institute of Astronautical Systems Engineering, Beijing 100076, China*

Correspondence should be addressed to Xunliang Yan; xly_nwpu@126.com

Received 21 August 2020; Revised 8 October 2020; Accepted 13 January 2021; Published 8 February 2021

Academic Editor: Paolo Castaldi

This paper focuses on the potential actuator failures of spacecraft in practical engineering applications. Aiming at the shortcomings and deficiencies in the existing attitude fault-tolerant control system design, combined with the current research status of attitude fault-tolerant control technology, we carry out high-precision, fast-convergent attitude tracking algorithms. Based on the adaptive nonsingular terminal sliding mode control theory, we design a kind of fixed-time convergence control method. This method solves the problems of actuator faults, actuator saturation, external disturbances, and inertia uncertainties. The control method includes control law design and controller design. The designed fixed-time adaptive nonsingular terminal sliding mode control law is applicable to the development of fixed-time fault-tolerant attitude tracking controller with multiple constraints. The designed controller considers the saturation of the actuator output torque so that the spacecraft can operate within the saturation magnitude without on-line fault estimation. Lyapunov stability analysis shows that under multiple constraints such as actuator saturation, external disturbances, and inertia uncertainties, the controller has fast convergence and has good fault tolerance to actuator fault. The numerical simulation shows that the controller has good performance and low-energy consumption in attitude tracking control.

1. Introduction

As my country continues to carry out deep-space missions such as the lunar exploration program and Mars exploration, the requirements for the stability, reliability, and autonomous operation capabilities of the entire spacecraft system, especially the spacecraft control system, have been significantly improved. As one of the subsystems of the spacecraft, the attitude control system plays an important role in the design of the spacecraft. Its reliability determines the success of the detection mission to a large extent. However, the long-term operation of orbiting spacecraft in harsh space environments such as strong radiation, high and low temperature, microgravity, and multiple disturbances, coupled with complex detection tasks, increases the possibility of failure of actuators, sensors, and controllers. According to foreign spacecraft's on-orbit attitude control system failure statistics, actuator and sensor failures accounted for 68% of the entire attitude control system failures, of which actuator failures accounted for 44% and sensor failures accounted for 24%. It is the existence of these practical engineering problems that greatly promote the reliability research of the attitude control system. Fault-tolerant control technology is an effective means to solve this problem without increasing the cost of system design. By designing reliable fault-tolerant control technology, the smooth implementation of space missions can be guaranteed [1–4]. In addition, energy is very important to spacecraft. How to save energy consumption in the process of spacecraft attitude control is the main concern of this article.

The sliding mode control (SMC) has good performance for nonlinear problems. By designing an appropriate SMC method, we can effectively handle nonlinear systems that have uncertainties, parameter disturbances, and bounded external disturbances. Therefore, SMC is widely applied to the attitude control of a spacecraft [5, 6]. Ref. [7] studied the problem of spacecraft attitude stabilization control system with limited communication and external disturbances based on an event-triggered control scheme. Ref. [8] designed an adaptive actuator fault and disturbance compensation method for attitude tracking control of spacecraft. This method is composed by a composite parameter adaptation design that includes an adaptive backstepping feedback control law and an adaptive feedforward actuator failure compensator. How to satisfy the control performance requirements under actuator failure and input saturation, Ref. [9] solve the problem of attitude tracking control with prescribed performance guarantees for a rigid spacecraft under unknown but constant inertia parameters, unexpected disturbances, actuator faults, and input saturation. Ref. [10] designed two fault-tolerant control (FTC) methods for spacecraft attitude stabilization with external disturbances. Ref. [11] solves the problem of finite-time fault-tolerant attitude stability control for rigid spacecraft under the conditions of actuator faults or failure, external disturbances, and modelling uncertainty. Ref. [12] studied the attitude tracking problem of rigid body with actuator faults and angular velocity constraints during the attitude maneuver. Ref. [13] proposed an adaptive fuzzy fault-tolerant attitude tracking controller. The controller can stabilize the attitude of the rigid spacecraft in the case of unavailable velocity, external disturbance, actuator faults, and actuator saturation. Using the nonlinear model, the predictive control method can predict the future behaviour of the system. Ref. [14] studied the translation-rotation-coupled motion problem for the control of an all-thruster spacecraft in the presence of actuators fault and/or failure. Ref. [15] presents a sliding mode control scheme with finite reaching time for a satellite fault-tolerant attitude control system with actuator fault and external disturbances. In Ref. [16], an active fault-tolerant control system is designed for spacecraft attitude control with actuator faults, fault estimation errors, and control input constraints. Ref. [17] built two observers to accurately estimate the uncertain kinematic and dynamic parameters. It is theoretically proved that the whole observer-controller system is globally exponentially stable. In reference [18], a class of flexible spacecraft attitude systems with the Lipschitz nonlinearity and sensor fault is studied for the problem of active fault-tolerant control (FTC). Ref. [19] presents a decoupling method to solve the integrated design problem of fault estimation (FE) and fault-tolerant control (FTC) for linear systems with unknown bounded actuator faults and disturbances. Ref. [20] studied a control system with additive faults and a controller with three blocks and calculated the fault-tolerant (FT) perfect tracking problem. In the control of nonlinear uncertain systems, compensating infinite number of actuator failures/faults with the well-known tuning function method is an important and challenging problem in the field of adaptive control. In Ref. [21], the problem of fault-tolerant control and closed-loop control allocation for spacecraft attitude control systems with actuator failure, actuator saturation, and external disturbances is solved. For fourth-order systems, Ref. [22] proposes an adaptive super-twisting decoupled terminal sliding mode control technique. Using the adaptive-tuning law can eliminate the requirements of upper bounds of external perturbations. By using super-twisting algorithm, the chattering phenomenon is avoided without affecting the control performance.

For actuator failure, under the assumption that the upper bound of the uncertainties is known, the existing literature has designed a high-precision, finite-time convergence attitude fault-tolerant control law. Although they can achieve high precision and stability of the attitude control system, they do not consider other control index requirements, and engineering application value. These attitude control methods still have the following two major problems to be further studied:

(1) It can only ensure that the two indexes of attitude control accuracy and stability are satisfied, and the index requirement of attitude maneuvering speed is not considered, and the latter is extremely critical to the space mission

(2) Only external disturbances and system uncertainties are considered, and actuator faults are not considered. These failures will have a significant impact on attitude control

(1) At present, most attitude control algorithms only consider the constraints of the control torque. Although the simulation results have verified the effectiveness of the attitude control algorithm, the energy consumption of the designed control algorithm is not analyzed and improved.

For the above defects, we need to design a new control law to solve the above problems. Inspired by Ref. [23], on the basis of Refs. [24, 25], this paper designed the fixed-time nonsingular terminal sliding mode (FNTSM) control law based on the parameter adaptive method. According to the Lyapunov stability theory, the system control law and adaptive parameter model are derived. The 4main contributions of this article are as follows:

(1) Low-energy consumption, this is the main contribution of the control method of this article: The control law designed in this paper has better characteristics compared with Ref. [24]. Specifically, the convergence time of the system is further reduced, the control saturation can be completely avoided, and less energy consumption is required

(2) The attitude convergence time is further reduced, and the performance of the control algorithm is further improved: Combining the design method of sliding mode surface and control law in the existing literature, this paper presents a new control law. Under the same initial conditions, the control law can have a faster convergence time for the system while maintaining high control accuracy.

The structure of this paper is as follows: "Materials and the Models for Tracking Spacecraft's Attitude" gives the attitude tracking control model under actuator failure and saturation. Using this control model, an adaptive control law is designed in "Designing the Fault-Tolerant Controller Law." In "Simulation Results Analysis," the designed control law is simulated and verified. "Conclusions" summarizes the analysis and follow-up prospects.

2. Materials and the Models for Tracking Spacecraft's Attitude

According to Refs. [3, 10–16, 24–27], the spacecraft attitude control system model with actuator faults and actuator saturation can be described by the following formula:

$$\begin{cases} q_{e0} = q_0 q_{d0} + \boldsymbol{q}_d^{\mathrm{T}} \boldsymbol{q} \\ \boldsymbol{q}_e = q_{d0} \boldsymbol{q} - q_0 \boldsymbol{q}_d + \boldsymbol{q}^{\times} \boldsymbol{q}_d, \end{cases} \tag{1}$$

$$\begin{aligned} \boldsymbol{J}_0 \dot{\boldsymbol{w}}_e = &-(\boldsymbol{w}_e + \boldsymbol{C}\boldsymbol{w}_d)^{\times} \boldsymbol{J}_0 (\boldsymbol{w}_e + \boldsymbol{C}\boldsymbol{w}_d) + \boldsymbol{J}_0 (\boldsymbol{w}_e^{\times} \boldsymbol{C}\boldsymbol{w}_d - \boldsymbol{C}\dot{\boldsymbol{w}}_d) \\ &+ \boldsymbol{D}\mathrm{sat}(\boldsymbol{u}_c) + \bar{\boldsymbol{d}}(t), \end{aligned} \tag{2}$$

where

$$\begin{aligned} \bar{\boldsymbol{d}}(t) = &-(\boldsymbol{w}_e + \boldsymbol{C}\boldsymbol{w}_d)^{\times} \Delta \boldsymbol{J} (\boldsymbol{w}_e + \boldsymbol{C}\boldsymbol{w}_d) + \Delta \boldsymbol{J} (\boldsymbol{w}_e^{\times} \boldsymbol{C}\boldsymbol{w}_d - \boldsymbol{C}\dot{\boldsymbol{w}}_d) \\ &- \Delta \boldsymbol{J} \dot{\boldsymbol{w}}_e + \boldsymbol{D}(\boldsymbol{E}(t) - \boldsymbol{I}_N)\boldsymbol{u}_c + \boldsymbol{D}\bar{\boldsymbol{u}}_c + \boldsymbol{d}(t), \end{aligned} \tag{3}$$

$$\mathrm{sat}\left(u_{c_i}\right) = \begin{cases} u_{c_i} & \left|u_{c_i}\right| < u_{\max} \\ u_{\max} \cdot \mathrm{sign}\ \left(u_{c_i}\right) & \text{otherwise}, \end{cases} \tag{4}$$

$$\begin{gathered} \Theta_i(u_{ci}(t)) = \begin{cases} 1 & \left|u_{c_i}\right| < u_{\max} \\ u_{\max}/u_{ci} \cdot \mathrm{sign}\ \left(u_{c_i}\right) & \text{otherwise}, \end{cases} \\ 0 < \delta \le \min\ (\Theta_i(u_{ci}(t))) \le 1, \end{gathered} \tag{5}$$

where δ is an unknown constant greater than zero.

Remark 1. The modelling process of this article refers to Refs. [24, 25, 27], and the detailed modelling process can be read in related literature. The specific meaning of the parameters in Formula (1) is detailed in Refs. [24, 25, 27]. Also, Formula (3) satisfies the following equation: $\|\bar{\boldsymbol{d}}(t)\| \le b(1 + \|\boldsymbol{w}\| + \|\boldsymbol{w}\|^2 + \|\boldsymbol{w}\|^p + \|\boldsymbol{w}\|^q + \|\boldsymbol{w}\|^{pq})$. In Addition, the assumptions used in this article are the same as those in Refs. [24, 25, 27], which will not be explained here.

3. Designing the Fault-Tolerant Controller Law

3.1. Controller Design

3.1.1. Step 1: Designing the Sliding Mode Surface. According to the error quaternion and the angular velocity error, the sliding mode surface chosen is as follows [23, 25, 28]:

$$\boldsymbol{S}_e = \boldsymbol{w}_e + \boldsymbol{S}_{au}, \tag{6}$$

where $\boldsymbol{S}_e \in \mathbf{R}^3$ is the sliding mode surface and $\boldsymbol{S}_{au} = [\mathrm{S}_{au1}, \mathrm{S}_{au2}, \mathrm{S}_{au3}]^{\mathrm{T}}$ is given by [23, 25, 28]

$$\boldsymbol{S}_{au} = \begin{cases} l_1 \boldsymbol{q}_{ev} + l_2 \mathrm{sig}(\boldsymbol{q}_{ev})^2 & \text{if} \bar{\mathbf{S}} \ne 0_{3\times1}, \|\boldsymbol{q}_{ev}\| \le \varepsilon \\ \alpha \mathrm{sig}(\boldsymbol{q}_{ev})^{g_1} + \beta \mathrm{sig}(\boldsymbol{q}_{ev})^{g_2} & \text{otherwise}, \end{cases} \tag{7}$$

where $\bar{\mathbf{S}} = \boldsymbol{w}_e + \alpha \mathrm{sig}(\boldsymbol{q}_{ev})^{g_1} + \beta \mathrm{sig}(\boldsymbol{q}_{ev})^{g_2}$. α, β, g_1, g_2 are positive constants, satisfying$0.5 < g_1 = f_1/f_2 < 1$, $g_2 = f_3/f_4 > 1$, $l_1 = 0.5\alpha\varepsilon^{g_1-1} + 0.5\beta\varepsilon^{g_2-1}$, $l_2 = 0.5\alpha\varepsilon^{g_1-2} + 0.5\beta\varepsilon^{g_2-2}$, and $f_1 < f_2, f_3 > f_4$ are positive odd numbers. ε is a small positive constant, for instance $\varepsilon = 0.001$.

Remark 2. According to Ref. [25], $g_1 \in (0.5, 1), g_2 > 1$, if $\varepsilon = 0.001$, l_2 is much bigger than l_1. Therefore, when $|\boldsymbol{q}_{ev}| \le \varepsilon$, $l_2 \mathrm{sig}(\boldsymbol{q}_{ev})^2$ has the same magnitude as $l_1 \boldsymbol{q}_{ev}$, so it is guaranteed that $l_2 \mathrm{sig}(\boldsymbol{q}_{ev})^2$ takes effect to drive quaternion errors converging fast to sliding mode. When $|\boldsymbol{q}_{ev}| > \varepsilon$, $\boldsymbol{S}_{au} = \alpha \mathrm{sig}(\boldsymbol{q}_{ev})^{g_1} + \beta \mathrm{sig}(\boldsymbol{q}_{ev})^{g_2}$, it is guaranteed that sliding surfaces $\boldsymbol{S}_e$ and $\bar{\boldsymbol{S}}$ have the same form.

According to Eq. (13)

$$\boldsymbol{J}_0 \dot{\boldsymbol{S}}_e = \boldsymbol{J}_0 \dot{\boldsymbol{w}}_e + \frac{\boldsymbol{J}_0}{2} \boldsymbol{F}_e (q_{e4} \boldsymbol{I}_3 + \boldsymbol{q}_{ev}^{\times}) \boldsymbol{w}_e, \tag{8}$$

where [25]

$$\boldsymbol{F}_e = \begin{cases} l_1 \boldsymbol{I}_3 + 2 l_2\ \mathrm{diag}\ (\mathrm{sign}\ (q_{evi}) q_{evi}) & \text{if}\ \bar{\mathbf{S}} \ne 0, \|\boldsymbol{q}_{ev}\| < \varepsilon \\ \alpha g_1\ \mathrm{diag}\ \left(\mathrm{sign}\ (q_{evi}) q_{evi}^{g_1 - 1}\right) + \beta g_2\ \mathrm{diag}\ \left(\mathrm{sign}\ (q_{evi}) q_{evi}^{g_2 - 1}\right) & \text{otherwise}. \end{cases} \tag{9}$$

Table 1: The main parameters of spacecraft [24].

Parameter	Value
Nominal moment of inertial	$J_0 = [20, 1.2, 0.9; 1.2, 17, 1.4; 0.9, 1.4, 15]\mathrm{kg}\cdot\mathrm{m}^2$
Uncertainties ΔJ	$\Delta J = 2\ \mathrm{diag}\ [\sin(0.3t), 2\cos(0.2t), \sin(0.1t)]\mathrm{kg}\cdot\mathrm{m}^2$
$Q(0)$	$Q(0) = [0.3, -0.2, -0.3, 0.8832]^{\mathrm{T}}$
$w(0)/(\mathrm{rad}\cdot s^{-1})$	$w(0) = [0.06, -0.04, 0.05]^{\mathrm{T}}\mathrm{rad/s}$
$w_d/(\mathrm{rad}\cdot \mathrm{s}^{-1})$	$w_d(t) = 0.05[\sin(0.01\pi t), \sin(0.02\pi t), \sin(0.03\pi t)]^{\mathrm{T}}\mathrm{rad/s}$
$Q_d(0)$	$Q_d(0) = [0.3, 0.2, 0.5, 0.7874]^{\mathrm{T}}$
$d(\mathrm{t})$	$d(t) = [0.1\sin(0.1t), 0.2\sin(0.2t), 0.3\sin(0.3t)]^{\mathrm{T}}\mathrm{N}\cdot\mathrm{m}$

Introducing Eq. (16) into Eq. (15), there is [24]:

$$\begin{aligned} J_0\dot{S}_e = &-(w_e + Cw_d)^{\times}J_0(w_e + Cw_d) + J_0(w_e^{\times}Cw_d - C\dot{w}_d) \\ &+ D\Theta u_c + \bar{d}(t) + \frac{J_0}{2}F_e(q_{e4}I_3 + q_{ev}^{\times})w_e. \end{aligned} \tag{10}$$

The approach law adopted in this paper is similar to that in Refs. [24, 25, 27], as shown in the following formula:

$$J_0\dot{S} = -K_1\mathrm{sig}^{\lambda}(S_e) - K_2\mathrm{sig}^{\gamma}(S_e). \tag{11}$$

Specific parameters can refer to Ref. [24]

3.1.2. Step 2: Designing the Control Law

Assumption 3. There are unknown constants $c_1 \geq 0$ and $c_2 \geq 0$, which make the following formulas hold [24]:

$$\begin{aligned} &\left\|-(w_e + Cw_d)^{\times}J_0(w_e + Cw_d) + J_0(w_e^{\times}Cw_d - C\dot{w}_d)\right\| \leq c_1, \\ &\left\|\frac{J}{2}F_e\cdot(q_{e4}I_3 + q_{ev}^{\times})w_e\right\| \leq c_2\|w_e\|. \end{aligned} \tag{12}$$

Lemma 4. *Consider the nonlinear system [25, 29]:*

$$\dot{x}(t) = f(x(t)), x(0) = 0, f(0) = 0, x \in \mathbb{R}^n. \tag{13}$$

Suppose that there is a Lyapunov function $V(x)$, and scalars $\alpha, \beta, p, q \in \mathbb{R}^+$, $p < 1$, $q > 1$, such that

$$\dot{V}(x) + \alpha V^p(x) + \beta V^q(x) \leq 0. \tag{14}$$

Then, the trajectory of this system is practical fixed-time stable, which means the convergence time is independent of the initial state, and the convergence time is given as [25] follows:

$$T \leq \frac{1}{\alpha(1-p)} + \frac{1}{\beta(q-1)}. \tag{15}$$

Theorem 5. *Consider the spacecraft systems (1), (2), (3), (4), and (5) and the designed sliding mode surface (6), the system trajectories will converge to the sliding mode surface in finite time with the following control law (17) [24]:*

$$\begin{aligned} u_c(t) = D^{\div}\Big(&-K_1 sig^{\lambda}(S_e) - K_2 sig^{\gamma}(S_e) \\ &- \frac{S_e}{\|S_e\|}\eta\hat{\delta}\left(\hat{c}_1 + \hat{c}_2\|w_e\| + \hat{b}\varphi\right)\Big). \end{aligned} \tag{16}$$

where $D^{\div} = D^T(DD^T)^{-1}$ is the right-pseudo inversion of matrix D, $\hat{c}_1$, $\hat{c}_2$, $\hat{b}$ and $\hat{\delta}$ are adaptive parameters, and $\varphi = 1 + \|w\| + \|w\|^2 + \|w\|^p + \|w\|^q + \|w\|^{pq}$. The adaptive updating law is designed as follows [24]:

$$\begin{aligned} \dot{\hat{\delta}} &= \mu_0\eta\delta\wedge^3\|S_e\|\left(\hat{c}_1 + \hat{c}_2\|w_e\| + \hat{b}\varphi\right), \\ \dot{\hat{c}}_1 &= \mu_1\|S_e\|, \\ \dot{\hat{c}}_2 &= \mu_2\|S_e\|\|w_e\|, \\ \dot{\hat{b}} &= \mu_3\|S_e\|\varphi, \end{aligned} \tag{17}$$

where μ_i, $i = 0, 1, 2, 3$, and $\eta > 1$ are design parameters.

3.1.3. Step 3: Proving the Stability

Proof. The following Lyapunov function is selected [24]:

$$V_1 = \frac{1}{2}S_e^{\mathrm{T}}J_0S_e + \frac{1}{2\mu_0}\tilde{\delta}^2 + \frac{1}{2\mu_1}\tilde{c}_1^2 + \frac{1}{2\mu_2}\tilde{c}_2^2 + \frac{1}{2\mu_3}\tilde{b}^2, \tag{18}$$

where $\tilde{\delta} = \delta - \delta\wedge^{-1}$, $\tilde{c}_1 = c_1 - \hat{c}_1$, $\tilde{c}_2 = c_2 - \hat{c}_2$, and $\tilde{b} = b - \hat{b}$.

According to reference [24], the derivative of V_1 is as follows (for proof details, please refer to [24]):

$$\begin{aligned} \dot{V}_1 \leq &-\delta\left(\frac{2}{\lambda_{\max}(J_0)}\right)^{(\lambda+1)/2}\left(\min(K_{1i}) - \left(\frac{L_1}{V_1}\right)^{(\lambda+1)/2}\right)V_1^{(\lambda+1)/2} \\ &-\delta\left(\frac{2}{\lambda_{\max}(J_0)}\right)^{(\gamma+1)/2}\left(\min(K_{2i}) - \left(\frac{L_1}{V_1}\right)^{(\gamma+1)/2}\right)V_1^{(\gamma+1)/2}, \end{aligned} \tag{19}$$

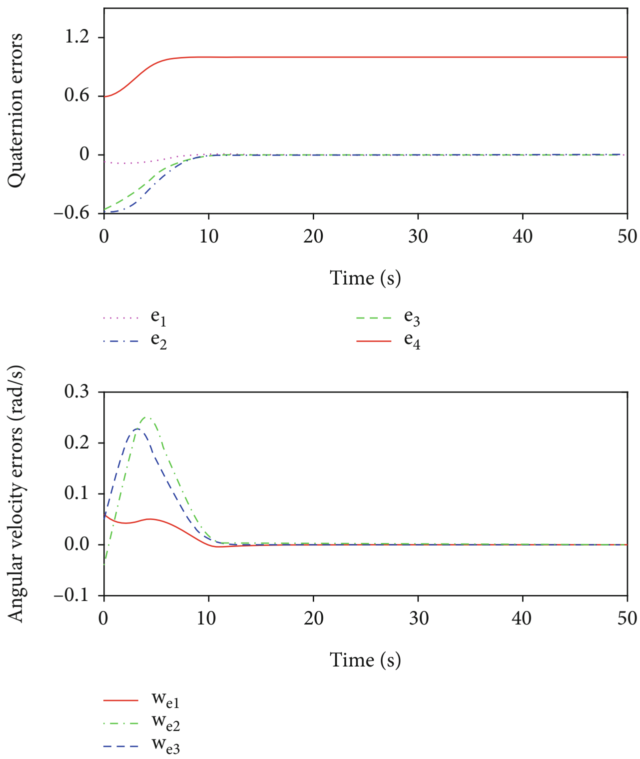

Figure 1: Time response of tracking errors.

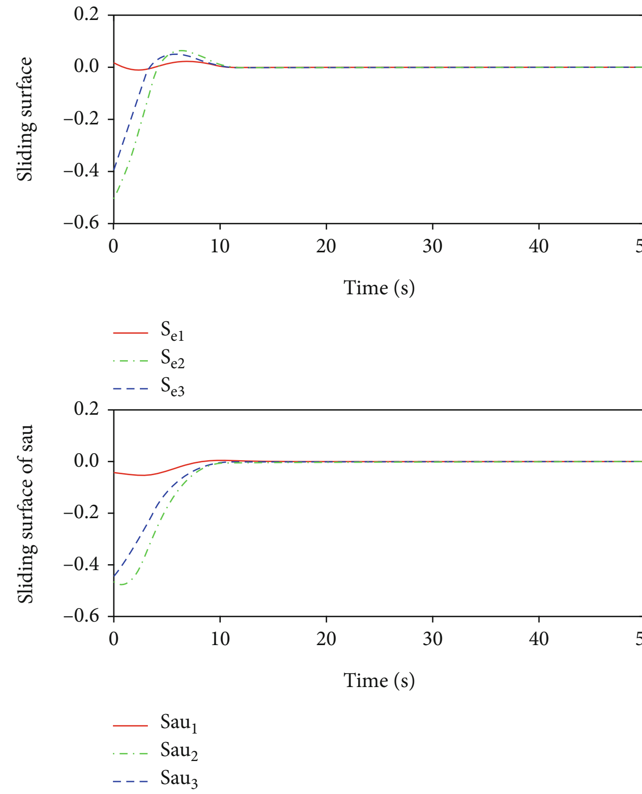

Figure 2: Time response of sliding surface and saturation sliding surface.

where $L_1 = (1/2\mu_0)\tilde{\delta}^2 + (1/2\mu_1)\tilde{c}_1^2 + (1/2\mu_2)\tilde{c}_2^2 + (1/2\mu_3)\tilde{b}^2$. And $L_1/V_1 < 1$, $(L_1/V_1)^{(\lambda+1)/2} < 1$, $(L_1/V_1)^{(\gamma+1)/2} < 1$ according to $L_1 < V_1$. If min $(K_{1i}) \geq 1$, min $(K_{2i}) \geq 1$, Expression (32) is simplified into $\dot{V}(x) + \alpha V^p(x) + \beta V^q(x)$; the spacecraft may undergo the faster finite time stability Condition (19) of Lemma 4 and can reach the sliding mode surface in fixed-time. Therefore, according to Lemma 4, the convergence time satisfies [24]

$$t_1 \leq \frac{1}{\chi_2(1-p)} + \frac{1}{\chi_1(q-1)}, \tag{20}$$

where $\chi_1 = \delta(2/\lambda_{\max}(\boldsymbol{J}_0))^{(\lambda+1)/2}(\min(K_{1i}) - (L_1/V_1)^{(\lambda+1)/2})$ and $\chi_2 = \delta(2/\lambda_{\max}(\boldsymbol{J}_0))^{(\gamma+1)/2}(\min(K_{2i}) - (L_1/V_1)^{(\gamma+1)/2})$, $p = \gamma + 1/2 < 1$, $q = \lambda + 1/2 > 1$.

Remark 6. When the system state reaches the sliding surface, the stability of the sliding surface itself is proved to be the same as that in the Ref. [25], and it is not described again.

Remark 7. The control algorithm designed in this paper includes many parameters, such as $\alpha, \beta, g_1, g_2, \varepsilon, \boldsymbol{K}_1, \boldsymbol{K}_2$. When selecting these parameters, firstly, the constraint conditions of the parameters need to be satisfied, and secondly, we adjust and optimize the parameters according to the relevant conclusions of the existing literature and the simulation results.

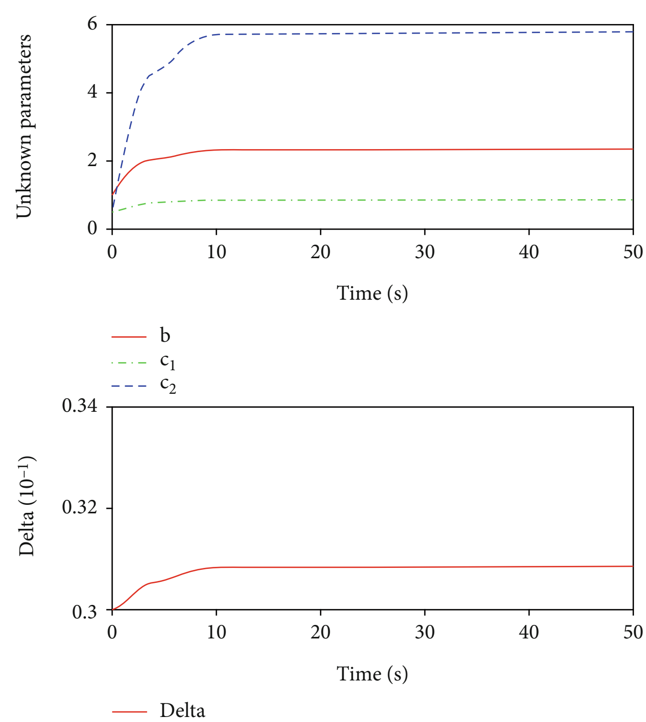

Figure 3: Time response of estimating unknown parameters and controller saturation.

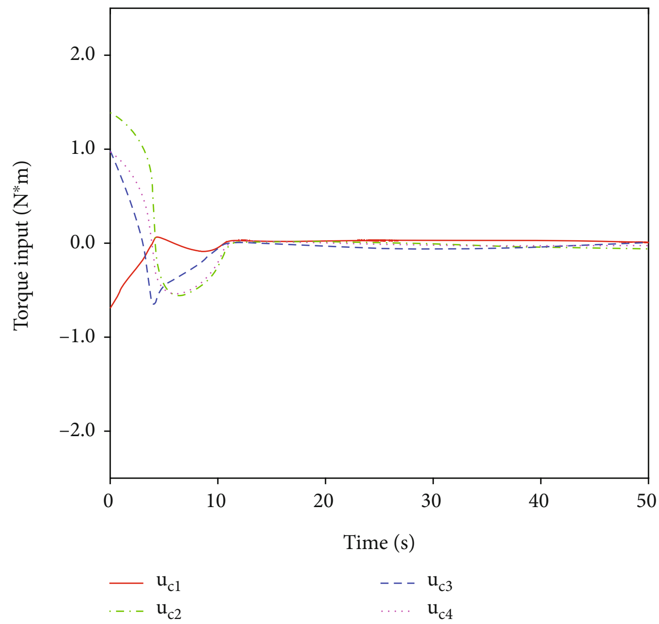

FIGURE 4: Time response of controlling torque.

Remark 8. Although the control algorithm designed in this paper includes many parameters, when designing parameters, selecting values according to the constraints of the parameters can basically achieve the expected control performance. In addition, through the analysis of the simulation results, the relevant parameters can be further optimized.

Remark 9. In the design of control law, the design idea of Ref. [24] and the sliding mode surface design method of Ref. [25] are used in this paper. In terms of design idea, Ref. [24] and Ref. [25] are combined. However, from the perspective of energy consumption, this paper proves the superiority of the combined controller, which is also the greatest contribution of this paper. The results of simulation analysis further support the greatest contribution of this paper.

4. Simulation Results Analysis

To illustrate the performance of the FNTSM law (17) proposed in this paper and compare it with the controller (25) in Ref. [24], we carry out the simulations. The spacecraft model is taken from a rigid-body microsatellite, and parameters are selected as follows (in this session, this paper uses the same simulation parameters as Ref. [24], in order to illustrate the great performance improvements of the control law proposed, compared with the one in Ref. [24], as mentioned in Table 1).

The actuator effective decline faults are [24]

$$E_i = \begin{cases} 1 & t \le 10 \\ 0.35 + 0.1 \sin\left(0.5t + \pi i/3\right) & t > 10. \end{cases} \tag{21}$$

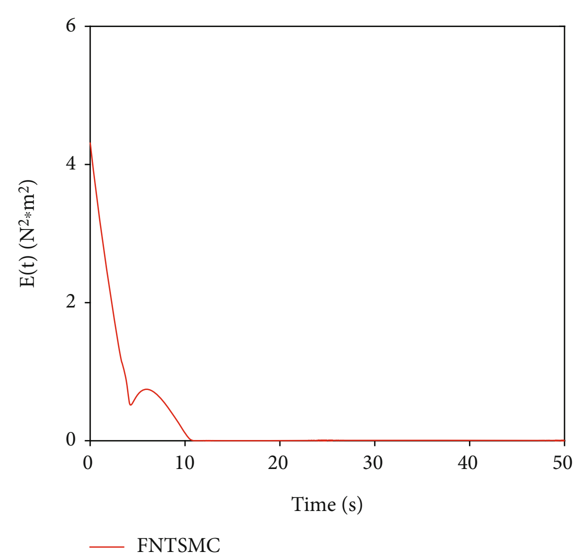

FIGURE 5: Time response of energy consumption.

The actuator drift faults are [24]

$$\bar{u}_{ci} = \begin{cases} 0 & t \le 15 \\ 0.1 + 0.05 \sin\left(0.5 i\pi t\right) & t > 15. \end{cases} \tag{22}$$

We illustrate the control property of the FNTSM control law (17) for the spacecraft under the inertia uncertainties and external disturbances and even consider its actuator faults and saturations. The parameters of the FNTSM control law (17) and the sliding mode (13) are the same as those in Refs. [24, 25].

Figure 1 depicts the response curves of quaternion errors and angular velocity errors. From Figure 1, we can see that

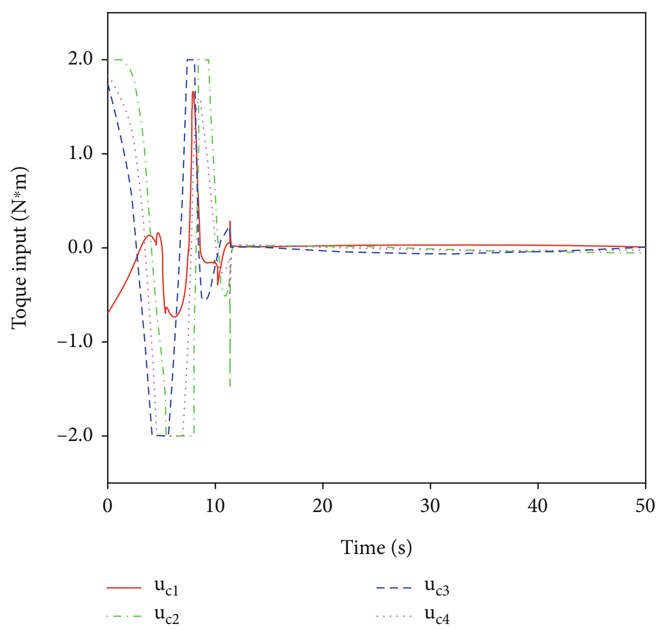

Figure 6: Time response of controlling torque in Ref. [24].

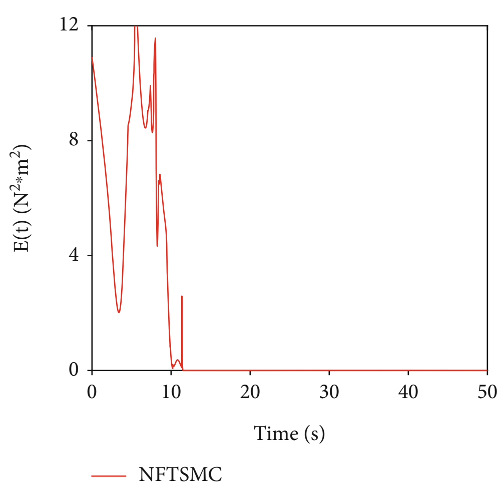

Figure 7: Time response of energy consumption in Ref. [24].

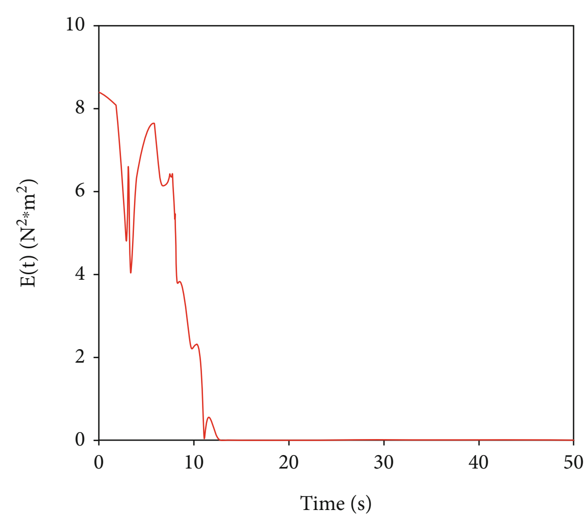

Figure 8: Time response of energy consumption by using the controller design idea in Ref. [27].

the control law designed in this paper has same performance as Ref. [24].

Figure 2 gives the response curves of sliding mode surface.

Figure 3 gives the estimated curves of uncertainty parameters and controller saturation. As Figure 3 (lower half) shows, the controller saturation curve hardly changes. Therefore, compared with the Ref. [24], the controller designed in this paper has better antisaturation performance.

Figure 4 shows the control torque curve. It can be seen from the figure that the system does not saturate during the entire control process.

Figure 5 shows the energy consumption curve of the system during the control process. It can be seen from the figure that the energy consumption at the initial moment is relatively large (about 4.1N^2m^2) but tends to zero quickly. In addition, the curve fluctuation is very small.

Figures 6 and 7 show the control torque curve and energy consumption curve obtained by the control law proposed in Ref. [24]. It can be seen from the Figure 6 that the control saturation of the system occurs in the first 10s, and the control torque curve fluctuates a lot. The energy consumption curve shows that the maximum energy consumption is about 3 times as much as that of the control law designed in this paper(about 12N^2m^2), and the fluctuation is relatively large during the control process. So compared with the control law designed in this paper, the control law in Ref. [24] has lower performance.

TABLE 2: The results on comparison of different controllers.

FNTSM control law performance	(17) in this paper	(25) in [24]
Quaternion error	$\pm 9.58 \times 10^{-4}$	$\pm 4.3 \times 10^{-5}$
Angular velocity error	$\pm 1.5 \times 10^{-4}$	$\pm 9.9 \times 10^{-6}$
FNTSM/NFTSM error	$\pm 9.88 \times 10^{-4}$	$\pm 8.5 \times 10^{-5}$
Convergence time(s)	9.97	11.01

By using the controller design idea in Ref [27] and combining the control object and model parameters in this paper, the energy consumption curve of the controller is shown in Figure 8.

Table 2 presents the results on the comparison of the FNTSM control law (17) with the controller (25) in Ref. [24]. As mentioned in Table 2 and illustrated in Figures 1–7, the FNTSM control law guarantees the steady precision in $|\boldsymbol{q}_{ev}| \leq 9.58 \times 10^{-4}$, $|\boldsymbol{w}_e| \leq 1.5 \times 10^{-4}$, and $|\boldsymbol{S}_e| \leq 9.88 \times 10^{-4}$, with the convergence time being 9.97 s. It can be seen that the control precision of the system is slightly reduced compared with Ref. [24] but still high enough. And the convergence time has increased by 10.43% compared with Ref. [24].

5. Conclusions

This paper designs an adaptive fault-tolerant control law, which can adapt to good control in the event of actuator faults. According to the simulation results, the control law designed in this paper has high control accuracy and fast tracking speed. At the same time, according to the control torque curve, the control law actuator designed in this paper does not saturate (all control forces are less than 2 Nm). In addition, comparing the simulation results shown in Figures 6–8, the control force designed in this paper consumes the least spacecraft energy during attitude tracking, which is very important for the orbiting spacecraft, which is also the biggest advantage of the control law in this paper.

6. Future Recommendation

According to the control law design process in this paper and the control law designed in the existing literature, the direction to further and improve the work main includes

(1) How to further improve the convergence time and control accuracy of the control algorithm

(2) How to further reduce the complexity of algorithm design

(3) Like the existing literature design method, how to reduce the related assumptions in algorithm design is a key issue that must be solved for the future development of spacecraft attitude control with high precision.

Conflicts of Interest

The authors declare that they have no conflicts of interest.

Acknowledgments

The authors would like to thank the referees for their valuable comments. The research is financially supported by the National Natural Science Foundation of China (No. 61502391, 11602296), the Natural Science Foundation of Shaanxi Province (Grant no. 2019JM-434), and Aviation Science Fund Project (No. 20180153002).

References

[1] A. M. Zanchettin, A. Calloni, and M. Lovera, "Robust magnetic attitude control of satellites," *IEEE/ASME Transactions on Mechatronics*, vol. 18, no. 4, pp. 1259–1268, 2013.

[2] Y. Yang, "Spacecraft attitude and reaction wheel desaturation combined control method," *IEEE Transactions on Aerospace and Electronic Systems*, vol. 53, no. 1, pp. 286–295, 2017.

[3] Y. Hamada, T. Ohtani, T. Kida, and T. Nagashio, "Synthesis of a linearly interpolated gain scheduling controller for large flexible spacecraft ETS-VIII," *Control Engineering Practice*, vol. 19, no. 6, pp. 611–625, 2011.

[4] B. Xiao, M. Huo, X. Yang, and Y. Zhang, "Fault-tolerant attitude stabilization for satellites without rate sensor," *IEEE Transactions on Industrial Electronics*, vol. 62, no. 11, pp. 7191–7202, 2015.

[5] L. Hui and J. Li, "Terminal sliding mode control for spacecraft formation flying," *IEEE Transactions on Aerospace and Electronic Systems*, vol. 45, no. 3, pp. 835–846, 2009.

[6] Z. Chen and J. Huang, "Attitude tracking and disturbance rejection of rigid spacecraft by adaptive control," *IEEE Transactions on Automatic Control*, vol. 54, no. 3, pp. 600–605, 2009.

[7] B. Wu, Q. Shen, and X. Cao, "Event-triggered attitude control of spacecraft," *Advances in Space Research*, vol. 61, no. 3, pp. 927–934, 2018.

[8] X. Yao, G. Tao, Y. Ma, and R. Qi, "Adaptive actuator failure compensation design for spacecraft attitude control," *IEEE Transactions on Aerospace and Electronic Systems*, vol. 52, no. 3, pp. 1021–1034, 2016.

[9] Q. Hu, X. Shao, and L. Guo, "Adaptive fault-tolerant attitude tracking control of spacecraft with prescribed performance," *IEEE/ASME Transactions on Mechatronics*, vol. 23, no. 1, pp. 331–341, 2018.

[10] Q. Shen, D. Wang, S. Zhu, and E. K. Poh, "Integral-type sliding mode fault-tolerant control for attitude stabilization of spacecraft," *IEEE Transactions on Control Systems Technology*, vol. 23, no. 3, pp. 1131–1138, 2015.

[11] Q. Shen, D. Wang, S. Zhu, and K. Poh, "Finite-time fault-tolerant attitude stabilization for spacecraft with actuator saturation," *IEEE Transactions on Aerospace and Electronic Systems*, vol. 51, no. 3, pp. 2390–2405, 2015.

[12] Q. Shen, C. Yue, C. H. Goh, B. Wu, and D. Wang, "Rigid-body attitude tracking control under actuator faults and angular velocity constraints," *IEEE/ASME Transactions on Mechatronics*, vol. 23, no. 3, pp. 1338–1349, 2018.

[13] B. Huo, Y. Xia, L. Yin, and M. Fu, "Fuzzy adaptive fault-tolerant output feedback attitude-tracking control of rigid spacecraft," *IEEE Transactions on Systems, Man, and Cybernetics: Systems*, vol. 47, no. 8, pp. 1898–1908, 2017.

[14] M. M. Tavakoli and N. Assadian, "Predictive fault-tolerant control of an all-thruster satellite in 6-DOF motion via neural

network model updating," *Advances in Space Research*, vol. 61, no. 6, pp. 1588–1599, 2018.

[15] Z. Gao, Z. Zhou, M. S. Qian, and J. Lin, "Active fault tolerant control scheme for satellite attitude system subject to actuator time-varying faults," *IET Control Theory & Applications*, vol. 12, no. 3, pp. 405–412, 2018.

[16] Q. Shen, C. Yue, C. H. Goh, and D. Wang, "Active fault-tolerant control system design for spacecraft attitude maneuvers with actuator saturation and faults," *IEEE Transactions on Industrial Electronics*, vol. 66, no. 5, pp. 3763–3772, 2019.

[17] B. Xiao and S. Yin, "Exponential tracking control of robotic manipulators with uncertain dynamics and kinematics," *IEEE Transactions on Industrial Informatics*, vol. 15, no. 2, pp. 689–698, 2019.

[18] Z. Gao, B. Han, G. Jiang, J. Lin, and D. Xu, "Active fault tolerant control design approach for the flexible spacecraft with sensor faults," *Journal of the Franklin Institute*, vol. 354, no. 18, pp. 8038–8056, 2017.

[19] J. Lan and R. J. Patton, "A decoupling approach to integrated fault-tolerant control for linear systems with unmatched non-differentiable faults," *Automatica*, vol. 89, pp. 290–299, 2018.

[20] J. D. Stefanovski, "Passive fault tolerant perfect tracking with additive faults," *Automatica*, vol. 87, pp. 432–436, 2018.

[21] B. Li, Q. Hu, G. Ma, and Y. Yang, "Fault-tolerant attitude stabilization incorporating closed-loop control allocation under actuator failure," *IEEE Transactions on Aerospace and Electronic Systems*, vol. 55, no. 4, pp. 1989–2000, 2019.

[22] D. A. Haghighi and S. Mobayen, "Design of an adaptive super-twisting decoupled terminal sliding mode control scheme for a class of fourth-order systems," *ISA Transactions*, vol. 75, pp. 216–225, 2018.

[23] B. Jiang, Q. Hu, and M. I. Friswell, "Fixed-time attitude control for rigid spacecraft with actuator saturation and faults," *IEEE Transactions on Control Systems Technology*, vol. 24, no. 5, pp. 1892–1898, 2016.

[24] Z. Han, K. Zhang, T. Yang, and M. Zhang, "Spacecraft fault-tolerant control using adaptive non-singular fast terminal sliding mode," *IET Control Theory and Applications*, vol. 10, no. 16, pp. 1991–1999, 2016.

[25] Z. Han, H. Fu, and F. Tian, "Adaptive fixed-time non-singular terminal sliding mode attitude stabilization control for rigid spacecraft with actuator faults," *International Journal of Computer and Electrical Engineering*, vol. 11, no. 3, pp. 155–163, 2019.

[26] M. Pyare, S. Janardhanan, and U. Mashuq, "Rigid spacecraft fault-tolerant control using adaptive fast terminal sliding mode," in *Advances and Applications in Sliding Mode Control Systems*, S. Brown, Ed., pp. 381–406, Springer Press, 2015.

[27] Z. Han, K. Zhang, and T. Yang, "Spacecraft attitude control using nonsingular finite-time convergence terminal sliding mode," in *2016 IEEE Chinese Guidance, Navigation and Control Conference (CGNCC)*, pp. 618–623, Nanjing, China, August 2016.

[28] K. Lu, *Research on Compound Control Design Methods for Spacecraft Attitude, [Ph.D. thesis]*, Beijing Institute of Technology, 2014.

[29] A. Polyakov, "Nonlinear feedback design for fixed-time stabilization of linear control systems," *IEEE Transactions on Automatic Control*, vol. 57, no. 8, pp. 2106–2110, 2012.